Charge correlation effects on ionization of weak polyelectrolytes



2009 J. Phys.: Condens. Matter 21 424113

(http://iopscience.iop.org/0953-8984/21/42/424113)

IOP Publishing Journal of Physics: Condensed Matter

J. Phys.: Condens. Matter **21** (2009) 424113 (7pp) doi:10.1088/0953-8984/21/42/424113

# Charge correlation effects on ionization of weak polyelectrolytes

**A Z Panagiotopoulos**

Department of Chemical Engineering and Institute for the Science and Technology of Materials, Princeton University, Princeton, NJ 08544, USA

E-mail: azp@princeton.edu

Received 20 March 2009, in final form 18 May 2009
Published 29 September 2009
Online at stacks.iop.org/JPhysCM/21/424113

**Abstract**

Ionization curves of weak polyelectrolytes were obtained as a function of the charge coupling strength from Monte Carlo simulations. In contrast to many earlier studies, the present work treats counterions explicitly, thus allowing the investigation of charge correlation effects at strong couplings. For conditions representing typical weak polyelectrolytes in water near room temperature, ionization is suppressed because of interactions between nearby dissociated groups, as also seen in prior work. A novel finding here is that, for stronger couplings, relevant for non-aqueous environments in the absence of added salt, the opposite behavior is observed—ionization is enhanced relative to the behavior of the isolated groups due to ion–counterion correlation effects. The fraction of dissociated groups as a function of position along the chain also behaves non-monotonically. Dissociation is highest near the ends of the chains for aqueous polyelectrolytes and highest at the chain middle segments for non-aqueous environments. At intermediate coupling strengths, dissociable groups appear to behave in a nearly ideal fashion, even though chain dimensions still show strong expansion effects due to ionization. These findings provide physical insights on the impact of competition between acid/base chemical equilibrium and electrostatic attractions in ionizable systems.

(Some figures in this article are in colour only in the electronic version)

## 1. Introduction

Polyelectrolytes are polymers that contain charged groups along their backbone or side groups. They are involved in industrial processes and are found in many consumer products. DNA and most proteins also contain ionizable groups; Coulombic interactions often play a key role in biological processes. For many polyelectrolyte systems, the presence or absence of charge on particular groups is a function of solution pH. The charging state of groups in these 'weak' (or 'annealed') polyelectrolytes is also influenced by the addition of salt, solution concentration and the conformational state of the chains, which in turn depends on solvent quality. In contrast, 'strong' (or 'quenched') polyelectrolytes carry permanent charges irrespective of solution conditions. Properties of both types of polyelectrolytes in solution and at interfaces have been extensively studied by simulation (e.g. [1–11]) and theoretical methods (e.g. [12–24]). Recent general reviews of polyelectrolyte theories are available [25–28], as well as surveys of experimental and theoretical aspects of titration curves for weak polyelectrolytes [29–31].

Several prior simulation studies exist of ionization curves for weak polyelectrolytes. Uyaver and Seidel [32] observed sharp transitions in the ionization degree and radius of gyration as a function of effective pH in a poor solvent and examined the formation of pearl-necklace structures near $\theta$ conditions [33] and the effects of added salt on the structure of the chains [34]. Ulrich *et al* [35] performed Monte Carlo simulations of chains with varying attractions between monomers. The ionization curves were observed to be different for the polymer relative to the isolated monomers because of the strong electrostatic interaction between nearby charges. This work was recently extended to include stiffness and blockiness effects on the conformations and titration curves [36]. Yamaguchi *et al* [37] performed simulations of the coil–globule transition for weak polyelectrolytes. These studies do not include explicit counterions and use the screened Coulomb potential to describe the effects of added salts, so that ion correlation effects resulting from strong interactions between opposite

 

charges are absent. The recent study of Kosovan *et al* [38] of weak polyelectrolyte conformations in a poor solvent takes into account counterions explicitly, but imposes a fixed total charge on the chain and is performed at a coupling strength for which counterion correlation effects are relatively weak.

The present work aims to investigate the effect of charge interactions and correlations on the ionization properties of weak polyelectrolytes in the low salt limit at which such effects are maximized due to the low level of screening. The main distinguishing features relative to prior simulation studies are the explicit treatment of counterions and the inclusion of cases for which the charge coupling strength is stronger than what is expected for aqueous electrolytes. Experimentally, strong charge coupling effects are relevant for ionization in non-aqueous media [39] or for the interior of biological structures in which the effective dielectric constant is believed to be significantly lower than for bulk water [40]. In order to restrict the number of variables, only the case of good solvent conditions is examined here.

## 2. Model and methods

The model used in the present study represents chains as self-avoiding random walks on a three-dimensional simple cubic lattice. The number of segments (beads) in a chain is denoted by $n$, while the total number of chains in the system is $N$. The lattice spacing, $l$, is taken as the unit of length. Bonds connecting successive monomers are along lattice vectors (0, 0, 1), (0, 1, 1) and (1, 1, 1) and their reflections with respect to the principal axes, for a total of $Z = 26$ possible orientations. The model originates in the work on lattice surfactants by Larson [41]; its phase and micellization behavior have been studied previously [42, 43]. The bond length between successive segments can be 1, $\sqrt{2}$ and $\sqrt{3}$ in units of $l$ and thus local segment moves are possible that do not violate chain connectivity constraints. Starting with the first segment, every $m$ segments are ionizable. To preserve symmetry of the chains with respect to the two ends, only values of $n$ for which the last segment is also ionizable have been studied here.

Ionizable segments exist in two states, one neutral and one with a negative charge, thus representing acidic polyelectrolytes such as polyacrylic acid. Ionization releases a positive charge to free solution, according to the reaction $\mathrm{AH} \rightleftarrows \mathrm{A}^- + \mathrm{H}^+$. The dissociation reaction equilibrium constant $K_\mathrm{a}$ is related to the standard Gibbs free energy change of the dissociation reaction, $\Delta G$, by

$$K_\mathrm{a} = \exp(-\beta \Delta G) \tag{1}$$

where $\beta = 1/k_\mathrm{B}T$ is the inverse temperature. The negative of the common logarithm of the equilibrium constant, $\mathrm{pK_a} = -\log_{10}(K_\mathrm{a})$, is used to characterize the acidity of ionizable groups. In the model, positive charges are represented explicitly as monomers with excluded-volume interactions with the rest of the system. Excluded-volume interactions are also present between all chain segments, charged and uncharged. Implicit solvent particles occupying 'empty' lattice sites do not interact with any segments, so the simulations correspond to good solvent conditions for the polymer. Two segments with charges $q_1$ and $q_2$ at distance $r$ interact via the Coulomb potential:

$$U = \frac{q_1 q_2}{4\pi\varepsilon\varepsilon_0 r} \tag{2}$$

where $\varepsilon_0$ is the dielectric permittivity of vacuum and $\varepsilon$ is the dielectric constant of the solvent. The unscreened potential is used because explicit counterions are present in the system; any screening effects arise naturally as the ions redistribute themselves in the course of the simulations. Electrostatic repulsions between immediately adjacent sites on the backbone (for $m = 1$) can result in bond stretching, which contributes to the overall increase of chain dimensions at intermediate couplings described in section 3.

The energy of interaction of two elementary charges at their distance of closest approach is used to non-dimensionalize the strength of the Coulombic interaction, so that the reduced coupling strength $\lambda$ is

$$\lambda = \frac{e^2}{4\pi\varepsilon\varepsilon_0 l k_\mathrm{B} T} = \frac{l_\mathrm{B}}{l} \tag{3}$$

where $e$ is the unit of elementary charge, $l$ has already been defined as the lattice spacing and the Bjerrum length is $l_\mathrm{B} = e^2/(4\pi\varepsilon\varepsilon_0 k_\mathrm{B} T)$. Typical values of these parameters for electrolytes in room-temperature water ($\varepsilon = 78$, $l = 0.36$ nm) are $\lambda = 2$ and $l_\mathrm{B} = 0.72$ nm; longer distances of closest approach between charges result in lower coupling strengths, while smaller dielectric constants (e.g. in organic or mixed solvents) result in higher coupling strengths.

Periodic boundary conditions were used for the simulations. The reduced simulation box length, $L^* = L/l$ was set to $L^* = 100$, which is more than twice the maximum radius of gyration of the chains under the conditions studied. With typical values of the chain length ($n = 65$) and number of chains in the system ($N = 20$), the total volume fraction of chains is quite low, $\varphi = 0.0013$. Additional runs for $L^* = 126$ and $L^* = 79$, corresponding to twice and one-half the volume of the $L^* = 100$ box were performed to check for finite-size effects. Results in boxes of different volume were found to be identical within simulation statistical uncertainties. Statistical uncertainties were calculated by dividing the production period of the runs into nine blocks and obtaining the standard deviation of the block averages. Electrostatic interactions were calculated using Ewald sums with 518 Fourier-space vectors, tin-foil boundary conditions at infinity and a real-space reduced damping parameter $\kappa = 5$. As in previous work [44], the Ewald-summed Coulomb interaction between any two sites on the lattice was precalculated at the beginning of each simulation and used with a simple array lookup operation, resulting in substantial savings of CPU time for the relatively modest number of charged sites present in the systems studied.

Starting configurations for the simulations were generated by placing $N$ chains randomly within the simulation box. The chains were created as self-avoiding non-overlapping random walks and were initially completely uncharged. Three types of Monte Carlo steps were attempted in a fixed ratio of 3:2:5, namely association/dissociation steps, chain reptations by $m$ segments (to preserve the identity of ionizable

groups) and local displacement motions of the chain segments. Chain reptations were performed using a simple (athermal) Rosenbluth growth algorithm [45]. Local displacements involved randomly selecting a segment and attempting to move it to one of the 26 neighboring lattice positions within reduced distances of up to $\sqrt{3}$. Acceptance of the local displacement moves was performed with the standard Metropolis acceptance condition, provided that the chain connectivity constraint was satisfied. In the association/dissociation steps, with equal probability, (a) an attempt was made to switch an undissociated dissociable site into a negative site on the chain and a free positive ion in a randomly selected location or (b) a randomly selected positive ion was deleted and a randomly selected dissociated site was replaced with a neutral site. The probability of acceptance of attempted dissociation steps, $P_{\text{diss}}$, was according to the reactive canonical ensemble criterion [46]:

$$P_{\text{diss}} = \min\left[1, \frac{N_{\text{u}} L^3}{(N_{\text{d}}+1)^2} \exp(\beta\Delta U - \beta\Delta G)\right] \qquad (4)$$

where $N_{\text{u}}$ is the number of undissociated dissociatable sites, $N_{\text{d}}$ is the number of existing dissociated sites (equal to the number of free positive ions in solution) and $\Delta G$ is the intrinsic free energy change for the dissociation reaction. The corresponding acceptance probability, $P_{\text{assoc}}$, for the association steps is

$$P_{\text{assoc}} = \min\left[1, \frac{N_{\text{d}}^2}{(N_{\text{u}}+1)L^3} \exp(\beta\Delta U + \beta\Delta G)\right]. \qquad (5)$$

The number of attempted Monte Carlo moves per chain segment was in the range $10^5$–$10^7$, with more moves per segment at higher coupling strengths. The CPU time required was a strong function of the number of charge sites present; for the more highly charged systems the total time for a typical run was approximately 1 CPU day on a single core of a 3 GHz Xeon processor.

## 3. Results and discussion

A key quantity of interest in weak polyelectrolyte systems is the degree of ionization (dissociation) of the chains as a function of solution pH. This quantity can be obtained experimentally by potentiometric titration. If the ionizable groups do not have significant interactions with each other and other charged entities in solution, the fraction of dissociated groups, $f$, is simply given by the 'ideal ionization curve' [16]:

$$f = \frac{1}{1 + 10^{\text{pK}_{\text{a}} - \text{pH}}}. \qquad (6)$$

Because of the way our systems are set up, only the combination pH–$\text{pK}_{\text{a}}$ can be varied independently, so all results are reported in terms of this quantity. Figure 1 shows the degree of dissociation as a function of pH–$\text{pK}_{\text{a}}$ for a number of systems at different coupling strengths, overall chain concentration, chain length and frequency of ionizable groups. The prediction of equation (6) (continuous line) is indeed closely observed over the whole range of solution pH values at $\lambda = 0.1$ (crosses), which corresponds to weak

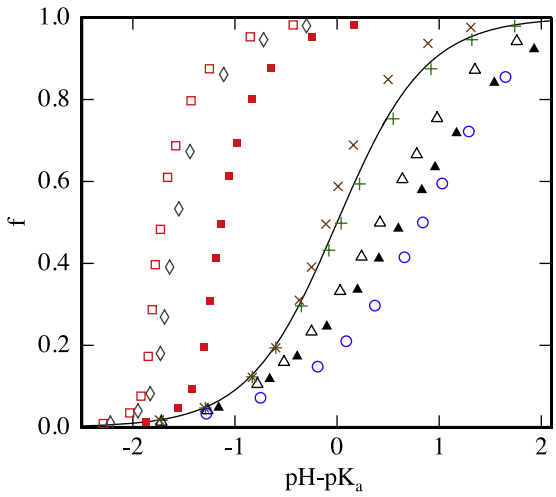


**Figure 1.** Degree of dissociation, $f$, versus pH–$\text{pK}_{\text{a}}$. The solid line is the ideal ionization expression of equation (6). Simulated systems have $n = 65$, $m = 4$, $N = 20$, unless otherwise noted. Points are as follows: (+) $\lambda = 0.1$; (Δ) $\lambda = 2$; (▲) $\lambda = 2$, $N = 5$; (○) $\lambda = 2$, $m = 1$; (×) $\lambda = 5.88$; (□) $\lambda = 10$; (■) $\lambda = 10$, $N = 5$; (◇) $\lambda = 10$, $n = 17$, $N = 50$. Statistical uncertainties are smaller than symbol size.

charge coupling. Even though only a single system with chain length $n = 65$, ionizable group frequency $m = 4$ and overall chain loading $N = 20$ is shown for $\lambda = 0.1$, similar results were obtained for other values of these parameters, as long as the coupling strength was sufficiently low. As suggested in the discussion following equation (3), values of the coupling strength $\lambda \leqslant 0.1$ correspond to large distances of closest approach between charges ($l \geqslant 7.2$ nm) for room-temperature aqueous systems. Another way to approach the ideal behavior, even at higher coupling strengths, is to increase the distance between ionizable groups—indeed, measurements of 'intrinsic' $\text{pK}_{\text{a}}$ values rely upon titration of the corresponding monomers in dilute solution.

Three sets of results are shown in figure 1 for $\lambda = 2$, a coupling strength corresponding to typical room-temperature aqueous polyelectrolytes. The chain length in all three cases was set to $n = 65$. Ionization curves at this coupling strength are shifted to higher pH values relative to the 'ideal' ionization relationship of equation (6), as seen previously in simulations with no explicit counterions [35]. The primary physical cause of this shift is the unfavorable interaction of nearby charges on the chain; ionization of a given group renders ionization of nearby groups less likely. There are no sharp discontinuities in the degree of ionization versus pH because the chains are in a good solvent, in contrast to the systems of [32, 37].

Increasing the amount of polyelectrolyte present from $N = 5$ (filled triangles) to $N = 20$ (open triangles) causes the ionization curves to shift nearer to the ideal curve, because of the increase in overall ionic strength of the solution. This effect of overall polymer loading is also seen experimentally at low salt concentrations [47], in simulations of counterion binding of strong polyelectrolytes [7] and in previous simulations of weak polyelectrolytes with no explicit counterions [35]. Decreasing the spacing of charged groups along the chains

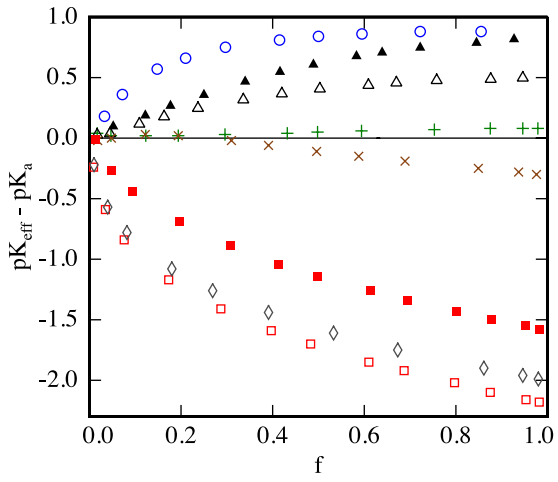


**Figure 2.** Effective ionization constant, $pK_{eff}$ versus degree of dissociation $f$. Symbols are as for figure 1. Statistical uncertainties are smaller than symbol size.

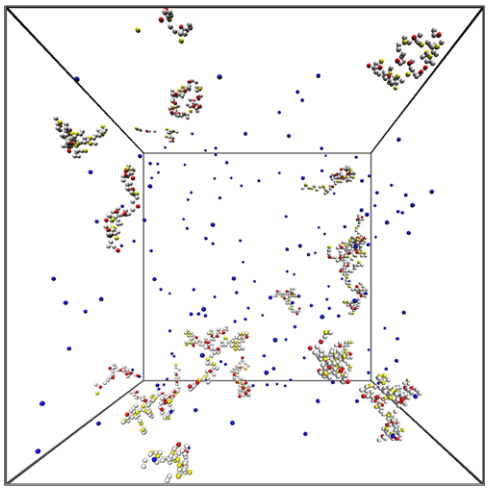

**Figure 3.** Snapshot from simulation at $\lambda = 0.1$, $n = 65$, $m = 4$, $N = 20$, $f = 0.49$. Undissociated segments are represented as white, uncharged dissociated segments are light gray (online: yellow), negatively charged segments are dark gray (online: red) and positive charges are black (online: blue).

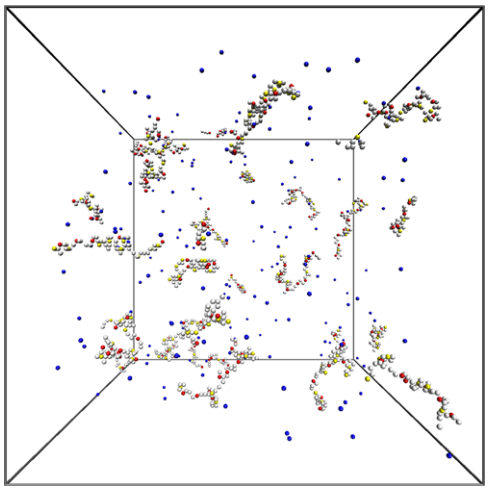

**Figure 4.** Snapshot from simulation at $\lambda = 2$, $f = 0.51$; other run parameters and color coding are as for figure 3.

(open circles, $m = 1$) results in a further strong shift of the ionization curves to higher pH values relative to $m = 4$, as expected on the basis of the increase in the magnitude of unfavorable charge–charge interactions along the chain backbone.

Another common way of representing experimental ionization data is shown in figure 2. The effective dissociation constant $pK_{eff}$ is defined as [30]

$$pK_{eff} = pH + \log \frac{1-f}{f}. \tag{7}$$

As can be seen in figure 2, for the low coupling strength case (crosses), the difference between effective and true ionization constants, $pK_{eff}$–$pK_a$, is nearly zero over the whole range of ionization, with small positive deviations near full ionization. Larger positive deviations for $\lambda = 2$ are primarily the result of interactions of nearby charges on the chains. These deviations become stronger for lower polymer concentrations and for closer spacing of the charges.

Interestingly, the ionization and $pK_{eff}$ curves become much closer to their near-ideal values when the coupling strength is increased further, as can be seen in figures 1 and 2 for $\lambda = 5.88$ (depicted by $\times$). This is particularly true at low degrees of dissociation—at higher degrees of dissociation, the ionization and $pK_{eff}$ curve are shifted to lower values. This trend continues at still higher coupling strengths, with a shift of the ionization to much lower pH values for $\lambda = 10$. Correspondingly, $pK_{eff}$ is now much lower than $pK_a$. This coupling strength corresponds to a medium of dielectric constant $\varepsilon = 16$. The effect of overall concentration of chains is in the same direction as before, with lower overall concentration ($N = 5$, filled squares) shifting the ionization curves to higher pH values relative to $N = 20$ (open squares). Decreasing the chain length to $N = 17$ (diamonds) also shifts the ionization curve to slightly higher pH values.

Before providing a physical explanation for the non-monotonic behavior of the overall ionization curves and discussing the local ionization and overall structure of the chains, it is helpful to examine some microscopic configurations that illustrate the major structural changes that take place in these systems as the coupling strength is increased. Figures 3–5 show the final configurations for runs at different values of $\lambda$, with other run parameters at common values of $n = 65$, $m = 4$, $N = 20$. For all cases the instantaneous degree of ionization is $f \approx 0.5$—since this is a fluctuating quantity, it is not possible to achieve precise control of its value for any specific configuration. Figure 3 at $\lambda = 0.1$ corresponds to nearly ideal behavior, figure 4 is at an intermediate $\lambda = 2$ and figure 5 is at the high value of $\lambda = 10$. The main large-scale visual differences between the three snapshots are (a) that chains are more extended at intermediate couplings and (b) that at the highest coupling there is a large degree of positive charge association with the negatively charged chains. Even though the total number of positive charges is approximately the same in all three

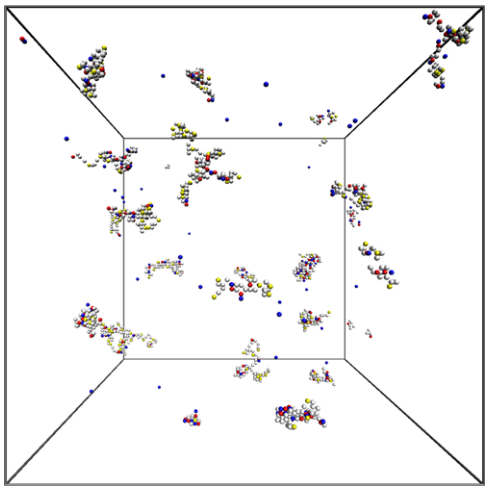

**Figure 5.** Snapshot from simulation at $\lambda = 10$, $f = 0.49$; other run parameters and color coding are as for figure 3.

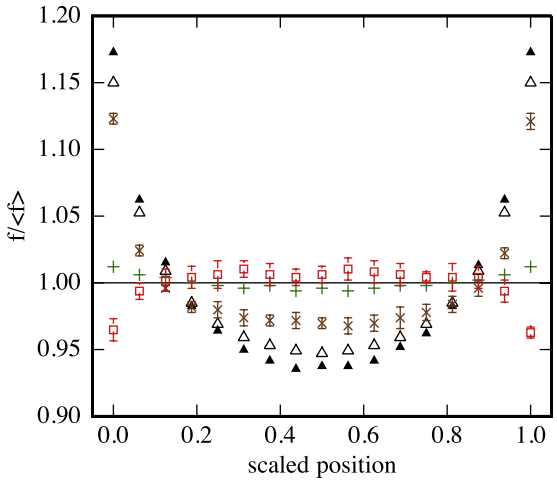


**Figure 6.** Local degree of dissociation versus scaled position along the chain. Symbols are as in figure 1, but for visual clarity only a subset of the conditions of figure 1 is plotted. Statistical uncertainties are shown only when greater than symbol size.

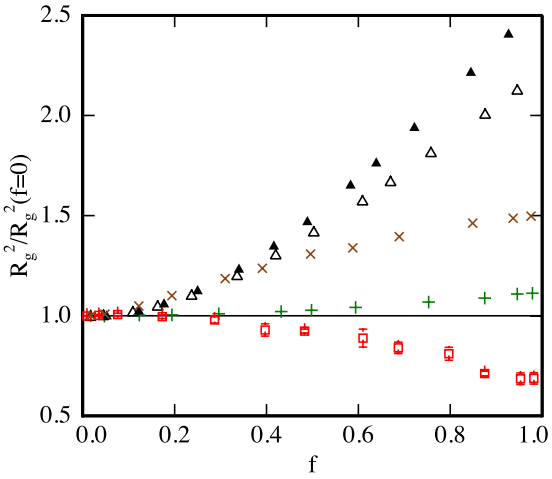


**Figure 7.** Normalized radius of gyration squared versus degree of dissociation $f$. Symbols are as in figure 1—for visual clarity, only a subset of the conditions of figure 1 are shown. Statistical uncertainties are shown only when greater than symbol size.

snapshots, most of them are closely associated with the chains in figure 5, rather than being free in solution as in figures 3 or 4. These strong charge correlation effects are, of course, not unique to weak polyelectrolytes—they are present in strong polyelectrolytes at sufficiently strong coupling strengths [1, 5].

The counterintuitive behavior of the ionization curves at high Coulomb coupling strengths can be understood as follows. For intermediate coupling strengths, for which nearby negatively charged groups on the chain interact unfavorably with each other, dissociation of a group suppresses dissociation of nearby groups and the overall ionization curves shift to higher pH values. In contrast, at high coupling strengths, nearby charged groups have effectively favorable (attractive) interactions through strong correlations with positive charges evident in figure 5 and seen previously for strong polyelectrolytes. At these conditions, dissociation of a segment attracts an opposite charge, the presence of which in turn *promotes* dissociation of nearby ionizable groups; the overall ionization curves shift to lower pH values and $pK_{eff}$ becomes significantly lower than $pK_a$. These effects become more pronounced as the degree of overall dissociation increases.

Theoretical analysis and simulations of annealed polyelectrolytes in good solvents [2, 14, 25] indicate that, at low coupling strengths, chain end segments are more charged than middle segments. Figure 6 illustrates this effect for the model systems, at conditions for which the mean overall degree of dissociation is $\langle f \rangle \approx 0.5$. At low coupling ($\lambda = 0.1$, depicted by crosses), the magnitude of the effect is small. At $\lambda = 2$, the chain ends carry approx. 15% higher charge than the average, while segments in the middle of the chains are 5% lower in degree of ionization than the average. Even at this coupling strength, the magnitude of the effect is relatively small, as seen previously [2, 14]. At $\lambda = 5.88$ (depicted by $\times$), a coupling strength at which the degree of ionization and effective $pK_a$ curves have reverted to near-ideal behavior, as seen in figures 1 and 2, the local degree of ionization is still of the same form as for lower coupling strengths, with middle segments less ionized than the ends. However, at higher couplings ($\lambda = 10$, squares) for which correlation effects are the strongest, the local degree of ionization shows the opposite behavior than previously, with the chain ends being *less* charged than segments near the middle of the chains. The origin of this reversal is again the strong charge correlation effects present at high coupling strengths. For low-to-intermediate coupling, negative charges along the chains effectively repel each other. Since association and dissociation provide an effective mobility (annealing) of charges along the backbone, this gives rise to the higher fraction of dissociated charges near the ends. In contrast, at high coupling strengths, negative charges along the chains effectively attract each other through interactions with the strongly correlated positive ions. This attraction leads to depletion of charge for the chain end segments.

Finally, chain dimensions are shown in figure 7, which depicts the mean-square radius of gyration normalized by its

value for the non-ionized chains plotted against the degree of dissociation $f$. At low coupling strengths ($\lambda = 0.1$, crosses), chain dimensions remain nearly equal to the value for non-ionized chains. At conditions corresponding to aqueous polyelectrolytes ($\lambda = 2$, triangles), there is a strong expansion of chain dimensions for the ionized chains because of repulsions along the backbone, as also seen in the snapshot of figure 4. This expansion is higher at lower overall polymer concentrations (filled triangles) which correspond to lower overall ionic strength. At $\lambda = 5.88$ (depicted by $\times$), dimensions for the ionized chains are still expanded relative to the non-ionized case, but less so than for $\lambda = 2$. However, at even higher coupling strengths ($\lambda = 10$, squares), chain dimensions contract as the degree of ionization is increased—this was indicated in the discussion of figure 5. As already mentioned, this non-monotonic dependence of chain dimensions on coupling strength is present for strong polyelectrolytes as well [1, 5]. It is the result of effective attractive interactions between similarly charged groups that originates in their mutual association with an ion of opposite charge; the same effective attraction between like charges also underlies ionic phase transitions in the restricted primitive model for ionic solutions [48]. A similar mechanism is operative in the multivalent salt-induced collapse of polyelectrolyte chain dimensions [8].

## 4. Concluding remarks

Simulations of systems of weak polyelectrolytes with explicit counterions have been shown here to be a promising approach for understanding charge correlation effects in these systems. Non-monotonic behavior of the degree of ionization as a function of solution pH was observed for coupling strengths greater than those corresponding to aqueous polyelectrolytes. These effects are in principle observable in pure or mixed solvents of lower dielectric constant than pure water. The fraction of dissociated groups at the ends of the chains also behaves non-monotonically, being greater for the end segments for aqueous polyelectrolyte systems and greater at the chain middle segments for non-aqueous ones. The degree of ionization is the first of these quantities to return to nearly ideal behavior, at conditions for which the chain dimensions are still expanded and the local degree of dissociation greater for the chain end segments. The physical origin of these observations is the effective attraction between like charges along the chains that is mediated by the strongly correlated counterions and that is also present in strong (fully ionized) polyelectrolytes. Another way to place these findings in context is to consider them as consequences of competition between acid/base chemical equilibrium and electrostatic attractions in ionizable systems. Minimization of the free energy in systems for low dielectric environments leads to a significant shift of acid/base equilibrium point in order to maximize favorable interactions between charges.

Several effects have not been systematically studied here and will be the subject of future work. In particular, the quality of the solvent has not been varied in the present study. There are strong effects on the degree of ionization of chain collapse due to solvophobic interactions [49]. Fluorescence measurements [50] indicate significant differences in local pH near the chains in a poor solvent that can also be investigated with the model proposed in the present study. Specific chemical interactions of the hydrated protons in real aqueous solutions are not taken into account in the present work and can be introduced in future versions of the model. Dissociation involving ions other than $H^+$ can also be modeled with only minor changes to the approach. Also, addition of salt with explicit representation of salt ions can be incorporated within the same modeling framework. Of particular interest are effects of multivalent counterions [51], which strongly couple to the polyelectrolyte charged groups. In many experimental systems, complex multistep curves of apparent pH are obtained as a function of the degree of ionization [29, 52]. These multistep transitions can be described by simple models with additional free parameters describing higher-order interactions between nearby groups [30] and are usually interpreted as resulting from conformational changes of the polymer. However, purely electrostatic interpretations of multistep titration curves are also available [29, 17] in which charge–charge correlations play a key role. It would be of interest to examine the relationships between chain microstructure and local degree of ionization in such systems. Finally, for grafted chains, the local pH and degree of dissociation are strong functions of position [20, 53–55]. The approach of the present work can also be used for detailed simulations of such systems at conditions that are challenging for current theoretical models.

## Acknowledgments

This work was supported by the National Science Foundation (MRSEC program) through the Princeton Center for Complex Materials (DMR 0819860). Addition support was provided by the US Department of Energy, Office of Basic Energy Sciences. I would like to thank Professor Igal Szleifer for useful comments and suggestions on this work.

## References

[1] Winkler R G, Gold M and Reineker P 1998 *Phys. Rev. Lett.* **80** 3731–4
[2] Zito T and Seidel C 2002 *Eur. Phys. J.* E **8** 339–46
[3] Liu S and Muthukumar M 2002 *J. Chem. Phys.* **116** 9975–82
[4] Jusufi A, Likos C N and Lowen H 2002 *J. Chem. Phys.* **116** 11011–27
[5] Orkoulas G, Kumar S K and Panagiotopoulos A Z 2003 *Phys. Rev. Lett.* **90** 048303
[6] Konieczny M, Likos C N and Lowen H 2004 *J. Chem. Phys.* **121** 4913–24
[7] Wang T Y, Lee T R, Sheng Y J and Tsao H K 2005 *J. Phys. Chem.* B **109** 22560–9
[8] Hsiao P Y and Luijten E 2006 *Phys. Rev. Lett.* **97** 148301
[9] Hehmeyer O J, Arya G, Panagiotopoulos A Z and Szleifer I 2007 *J. Chem. Phys.* **126** 244902
[10] Hsiao P Y 2008 *J. Phys. Chem.* B **112** 7347–50
[11] Lee H and Larson R G 2009 *Molecules* **14** 423–38
[12] Raphael E and Joanny J F 1990 *Europhys. Lett.* **13** 623–8
[13] Barrat J L and Joanny J F 1996 *Adv. Chem. Phys.* **94** 1–66
[14] Castelnovo M, Sens P and Joanny J F 2000 *Eur. Phys. J.* E **1** 115–25

[15] Deserno M, Holm C and May S 2000 *Macromolecules* **33** 199–206
[16] Netz R R 2003 *J. Phys.: Condens. Matter* **15** S239–44
[17] Burak Y and Netz R R 2004 *J. Phys. Chem.* B **108** 4840–9
[18] Wang Q, Taniguchi T and Fredrickson G H 2004 *J. Phys. Chem.* B **108** 6733–44
[19] Bizjak A, Rescic J, Kalyuzhnyi Y V and Vlachy V 2006 *J. Chem. Phys.* **125** 214907
[20] Gong P, Wu T, Genzer J and Szleifer I 2007 *Macromolecules* **40** 8765–73
[21] Kuhn P S, Levin Y, Barbosa M C and Ravazzolo A P 2007 *Macromolecules* **40** 7372–7
[22] Jeon J and Dobrynin A V 2007 *Macromolecules* **40** 7695–706
[23] Kundagrami A and Muthukumar M 2008 *J. Chem. Phys.* **128**
[24] de la Cruz M O, Ermoshkin A V, Carignano M A and Szleifer I 2009 *Soft Matter* **5** 629–36
[25] Holm C, Joanny J F, Kremer K, Netz R R, Reineker P, Seidel C, Vilgis T A and Winkler R G 2004 *Adv. Polym. Sci.* **166** 67–111
[26] Dobrynin A V and Rubinstein M 2005 *Prog. Polym. Sci.* **30** 1049–118
[27] Boroudjerdi H, Kim Y W, Naji A, Netz R R, Schlagberger X and Serr A 2005 *Phys. Rep.* **416** 129–99
[28] Dobrynin A V 2008 *Curr. Opin. Colloid Interface Sci.* **13** 376–88
[29] Borukhov I, Andelman D, Borrega R, Cloitre M, Leibler L and Orland H 2000 *J. Phys. Chem.* B **104** 11027–34
[30] Borkovec M, Koper G J M and Piguet C 2006 *Curr. Opin. Colloid Interface Sci.* **11** 280–9
[31] Marcus Y and Hefter G 2006 *Chem. Rev.* **106** 4585–621
[32] Uyaver S and Seidel C 2003 *Europhys. Lett.* **64** 536–42
[33] Uyaver S and Seidel C 2004 *J. Phys. Chem.* B **108** 18804–14
[34] Uyaver S and Seidel C 2009 *Macromolecules* **42** 1352–61
[35] Ulrich S, Laguecir A and Stoll S 2005 *J. Chem. Phys.* **122** 094911
[36] Ulrich S, Seijo M and Stoll S 2007 *J. Phys. Chem.* B **111** 8459–67
[37] Yamaguchi T, Kiuchi T, Matsuoka T and Koda S 2005 *Bull. Chem. Soc. Japan* **78** 2098–104
[38] Kosovan P, Limpouchova Z and Prochazka K 2008 *Collect. Czech. Chem. Commun.* **73** 439–58
[39] Rondinini S 2002 *Anal. Bioanal. Chem.* **374** 813–6
[40] Nyiri J and Noszal B 2005 *J. Solut. Chem.* **34** 1227–33
[41] Larson R G 1988 *J. Chem. Phys.* **89** 1642–50
[42] Panagiotopoulos A Z, Wong V and Floriano M A 1998 *Macromolecules* **31** 912–8
[43] Floriano M A, Caponetti E and Panagiotopoulos A Z 1999 *Langmuir* **15** 3143–51
[44] Panagiotopoulos A Z and Kumar S K 1999 *Phys. Rev. Lett.* **83** 2981–4
[45] Rosenbluth M N and Rosenbluth A W 1955 *J. Chem. Phys.* **23** 356–9
[46] Johnson J K, Panagiotopoulos A Z and Gubbins K E 1994 *Mol. Phys.* **81** 717–33
[47] Nagasawa M, Murase T and Kondo K 1965 *J. Phys. Chem.* **69** 4005–12
[48] Orkoulas G and Panagiotopoulos A Z 1994 *J. Chem. Phys.* **101** 1452–9
[49] Dubin P and Strauss U P 1973 *J. Phys. Chem.* **77** 1427–31
[50] Wang S Q, Granick S and Zhao J 2008 *J. Chem. Phys.* **129**
[51] Kotin L and Nagasawa M 1962 *J. Chem. Phys.* **36** 873
[52] Delben F, Paoletti S, Porasso R D and Benegas J C 2006 *Macromol. Chem. Phys.* **207** 2299–310
[53] Tagliazucchi M, Calvo E J and Szleifer I 2008 *Langmuir* **24** 2869–77
[54] Gong P, Genzer J and Szleifer I 2007 *Phys. Rev. Lett.* **98** 018302
[55] Nap R, Gong P and Szleifer I 2006 *J. Polym. Sci.* B **44** 2638–62